# Mitigating speckle noise in a laser Doppler vibrometer using Fourier analysis

Jin, Yang; Li, Zili

**DOI**
10.1364/OL.456040

**Publication date**
2022

**Document Version**
Final published version

**Published in**
Optics Letters

Optics Letters

# Mitigating speckle noise in a laser Doppler vibrometer using Fourier analysis

YANG JIN* AND ZILI LI

*Railway Engineering, Delft University of Technology, Postbus 5, 2600 AA, Delft, The Netherlands*
**Corresponding author: J.Jin-3@tudelft.nl*

*Received 14 February 2022; revised 29 July 2022; accepted 22 August 2022; posted 23 August 2022; published 9 September 2022*

**We propose two strategies for eliminating the speckle noise in a laser Doppler vibrometer according to Fourier analysis. Fourier transform is theoretically conducted on the speckle pattern phases, whose variation dominantly contributes to the speckle noise. The calculated and experimental frequency spectra of speckle noise both present oscillations of the frequency series (frequency peaks have constant intervals). (1) A low-pass filter can remove the noise if the vibration frequency is far lower than the first frequency peak of the noise. (2) The vibration energy can be revealed by removing the oscillating frequency trend. Physical experiments demonstrate the effectiveness of both despeckling strategies.** 

https://doi.org/10.1364/OL.456040

**Introduction**. A laser Doppler vibrometer (LDV) is an optical instrument extensively applied for noncontact vibration measurement [1–3]. Superior to attaching transducers, the LDV offers remote vibrometry (e.g., from a high-temperature surface) and avoids mass-loading undesired for light structures [4]. Precise measurements in time and frequency domains are available [5], as an LDV achieves a measuring frequency of 1 GHz and spatial resolution of 1 mm/s. In addition, the LDV on moving platforms (LDVom) [6] can one-way continuously scan a vibrating surface and monitor structures, especially those that are large or long like railway tracks.

A significantly issue of concern, speckle noise [7,8], that continuously buries vibration signals becomes extremely troublesome in LDVom signals. The signal drop-outs can exceed 40 times the vibration amplitude, and the dominant noise reduces the signal-to-noise ratio (SNR) to −15 db [9]. With periodic scanning, the speckle noise becomes pseudorandom, as its components centralize at the scanning frequency and distribute in the relevant harmonics [10]. It is convenient to handle this situation by avoiding the coincidence of the scanning and vibration frequencies [11]. The difficulty in noise removal increases in one-way scanning, as the noise randomly distributes in time and frequency domains. Thus classic signal processing approaches, such as bandpass filters and wavelet transform, lose their denoising effects without additional strategies. Numerous methods for eliminating speckle noise have been developed in recent researches; however, they are inappropriate for handling LDVom signals. For example, calculating the vibration energy can average the noise effect and identify defect locations [12,13], but disregards the waveforms crucial to modal analysis. The moving average approach [14] requires a scanning frequency much larger than the vibration frequency. Enhancing the surface reflection can mitigate the speckle noise [15] but is inapplicable in large-scale measurements. Physical characteristics of the speckle noise can inform despeckling procedures and thus should arouse research interest.

An optical phenomenon, laser speckle patterns produced by coherent laser beams scattering from an optically rough surface, is the origin of the LDV speckle noise [10]. The surface deviations at the laser-wavelength scale induce variant phases of incident wavelets. The reflected wavelets interfere constructively or destructively, producing bright or dark spots that constitute a speckle pattern. This generates intense noise when the photodetector translates or deforms. Statistical analysis and Fourier analysis have been utilized to characterize the speckle patterns [16–19]; but to our best knowledge, most former researches concentrated on the light intensity, contrast, and relationships with surface roughness. The variation of the resultant phase in the photodetector dominantly contributes to the speckle noise, but the relevant theoretical analysis stagnates in the simplified statistical properties. Fourier analysis can characterize the noise spectrum and promote corresponding despeckle approaches, which should be subjected to research.

In this Letter, we propose two novel strategies for eliminating the speckle noise in LDVom signals according to Fourier properties. Fourier analysis is theoretically conducted on the variation of the speckle phases. The despeckling approaches are developed according to the derived frequency spectrum and then evaluated with physical experiments.

**Method**. An LDV acquires a surface vibration according to the Doppler frequency shift. The principal optical element of an LDV is an electronic interferometer, where the reference laser beam is coherent with that diffusely reflected from the rough surface. The difference between the detected and reference laser frequencies ($f_d$ and $f_r$) derives the measured vibration velocity $v_m$ [20]:

$$v_m = \frac{\lambda}{2}(f_r - f_d) = \frac{\lambda}{4\pi}\left(2\pi f_r - \frac{d\varphi_d}{dt}\right) = v - \frac{\lambda}{4\pi}\frac{d\varphi_{res}}{dt}, \quad (1)$$

where $\varphi_d = 2\pi(f_r t - 2vt/\lambda + \varphi_{res}/2\pi)$ is the detected laser phase and $\lambda$ is the laser wavelength. The acquired vibration $v_m$ deviates from the true vibration $v$ by the phase variation $-\lambda d\varphi_{res}/(4\pi dt)$, namely the LDV speckle noise. The resultant phase $\varphi_{res}$ arises

from the laser speckle patterns illuminated inside the photodetector. Therefore, the variation of speckle patterns relevant to photodetector translation produces unwanted speckle noise. A speckle pattern $\mathcal{P}$ is the phasor summation of the coherent wavelets reflected from a rough surface [20]:

$$\mathcal{P} = \sum_{n=1}^{N} a_n e^{j\phi_n} = \mathcal{R} + j\mathcal{I}, \tag{2}$$

where $N$ is the number of scattered wavelets, $a_n$ is the wavelet amplitude, $\phi_n$ is the wavelet phase, $j$ represents the imaginary unit, and $\mathcal{R}$ and $\mathcal{I}$ represent real and imaginary parts, respectively. The phase $\varphi = \tan^{-1}\mathcal{I}/\mathcal{R}$ and intensity $I = \mathcal{R}^2 + \mathcal{I}^2$ of the speckle pattern approximately obey the uniform and exponential distributions, respectively [20]. Considering that the transmission laser illuminates $\kappa$ speckle patterns (each with phase $\varphi_s(\alpha,\beta)$ and intensity $I_s(\alpha,\beta)$, where $(\alpha,\beta)$ is the coordinate) and the reference beam retains the original phasor, the resultant phase $\varphi_{res}$ can be expressed as [20]

$$\tan\varphi_{res} = \frac{\sum_\alpha \sum_\beta \sqrt{I_s(\alpha,\beta)}\sin(\varphi_s(\alpha,\beta)-\varphi_r)}{\sum_\alpha \sum_\beta \sqrt{I_s(\alpha,\beta)}\cos(\varphi_s(\alpha,\beta)-\varphi_r)}, \tag{3}$$

where $\varphi_r$ is the phase of the reference beam. Fourier analysis provides the frequency spectrum for characterizing the signals and mitigating the noise. The Fourier transform on the speckle noise can be conducted as

$$\begin{aligned} F(\omega) &= \mathcal{F}\left(-\frac{\lambda}{4\pi}\frac{d\varphi_{res}}{dt}\right) = -j\frac{\lambda\omega}{4\pi}\mathcal{F}(\varphi_{res}) = -j\frac{\lambda\omega}{4\pi}\mathcal{F}(\sin^{-1}(x)) \\ &= -j\frac{\lambda\omega}{4\pi}\mathcal{F}\left(\sum_0^\infty \frac{(2n-1)!!}{(2n)!!}\frac{x^{2n+1}}{2n+1}\right), \end{aligned} \tag{4}$$

where $F(\omega)$ is the frequency function, $x = \sin\varphi_{res}$ is derived from Eq. (3), $\mathcal{F}$ represents the Fourier transform, $\omega = 2\pi f/f_s$ is the angular frequency, $f$ is the ordinary frequency, and $f_s$ is the sampling frequency. The last expression in Eq. (4) uses the Maclaurin series. The modulus $|F(\omega)|$ represents the frequency spectrum with its calculation related to the autocorrelation function. During LDV scanning, the neighboring-sampled spots share numerous overlapped speckle patterns, which enhance the autocorrelation property. Assuming an infinite scanning series with random speckle patterns, the autocorrelation function of $\sin^{-1}(x)$ is written as

$$\begin{aligned} R_{\varphi,\varphi}(t) =& R_{\varphi,\varphi}\left[\sum_0^\infty \frac{(2n-1)!!}{(2n)!!}\frac{x^{2n+1}}{2n+1}\right] \\ =& \sum_{p,q} C_{p,q}\frac{1}{\bar{I}_s^{p+q}} E\left(\left(\sum \sin(\varphi_s(\alpha,\beta)-\varphi_r)\right)^p\right. \\ & \left.\times\left(\sum \sin(\varphi_s(\alpha+v_s t,\beta)-\varphi_r)\right)^q\right) \\ =& \sum_{p,q} C_{p,q}\frac{1}{\bar{I}_s^{p+q}}\left(E\left(\sum_k \sin^{p+q}(\varphi_{s_k}-\varphi_r)\right)\right. \\ & \left.+E\left(\sum_e\prod_{b=1}^{p+q}\sin(\varphi_{s_{e,b}}-\varphi_r)\right)\right) \\ =& \sum_{p,q} C_{p,q}\frac{1}{(2\bar{I}_s)^{p+q}}\begin{matrix}p+q\\(p+q)/2\end{matrix}\frac{\kappa}{\pi L^2} \\ & \times\left(2L^2\cos^{-1}\left(\frac{v_s t}{L}\right) - 2\sqrt{v_s^2 t^2(L^2-v_s^2 t^2)}\right), \end{aligned} \tag{5}$$

where $\bar{I}_s$ is the $I_s$ average, $v_s$ is the scanning speed (the speed of the focusing spot moving on the target surface; assumed along the direction of $\alpha$), $E(\cdot)$ calculates the statistical expected value, $\sum_k \cdot$ represents the summation on overlapped speckles between the positions of $(\alpha,\beta)$ and $(\alpha+v_s t,\beta)$, $\sum_e \cdot$ represents the other summations, $L$ is the diameter of the focusing spot, $C_{p,q} = ((p-2)!!(q-2)!!)/(pq(p-1)!!(q-1)!!)$, and $p,q$ are odd. The component $E(\sum_e \prod_b \cdot)$ equals 0 for an infinite time series according to the uniform distribution of $\varphi_s$, while the component $E(\sum_k \cdot)$ is proportional to the overlapped spot area between time 0 and $t$. The last expression of Eq. (5) is based on $t \le L/v_s$, and $R_{\varphi,\varphi}(t)$ equals 0 with $t > L/v_s$ because of no overlapped speckle patterns. Therefore, the frequency spectrum can be written as

$$\begin{aligned} |F(\omega)| &= \frac{\lambda\omega}{4\pi}\sqrt{|\mathcal{F}(R_{\varphi,\varphi}(t))|} \\ &= \frac{\lambda\kappa\omega}{4\pi^2 L^2}\sqrt{\xi\left|\mathcal{F}\left(2L^2\cos^{-1}\left(\frac{v_s t}{L}\right) - 2L^2\sqrt{\left(\frac{v_s t}{L}\right)^2\left(1-\left(\frac{v_s t}{L}\right)^2\right)}\right)\right|} \\ \xi &= \sum_{p,q} C_{p,q}\frac{1}{(2\bar{I}_s)^{p+q}}\begin{matrix}p+q\\(p+q)/2,\end{matrix}\quad p,q \text{ are odd.} \end{aligned} \tag{6}$$

Equation (6) provides the significant curve trend of the speckle-noise spectrum, and the actual spectrum should contain fluctuations owing to the finite scanning series. Figure 1 illustrates both the theoretical and the experimental trends of the frequency spectrum. The frequency curve calculated by Eq. (6) oscillates with constant intervals (1024 Hz) between frequency peaks. With physical experiments, the trend of the frequency curve also presents constant intervals (820 Hz) between the frequency peaks. The experimental spectrum does not present an increasing trend because of the residual low-frequency vibration of the structure. The interval between frequency peaks is theoretically $v_s/L$ in Eq. (6), but the physical meaning of this value still needs investigation. According to this property, two strategies can be developed to mitigate the speckle noise: (1) a low-pass filter (LPF) is enough if the vibration frequency is far lower than the first frequency peak $v_s/2L$ and (2) adaptively removing the oscillation trend from the frequency spectrum can reveal the actual vibration energy. The trend of the frequency curve in a short window $f \in [f_\tau - f_0, f_\tau + f_0]$ approximates a sinusoid; thus, Eq. (7) provides an optimization method to pointwisely fit the

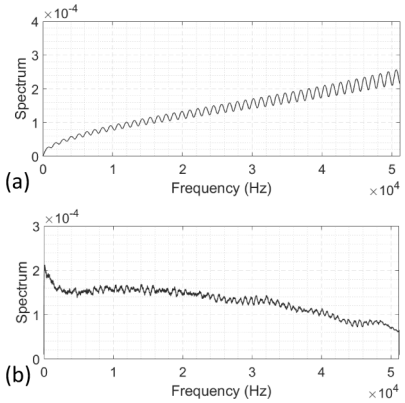


**Fig. 1.** (a) Frequency spectrum trend of the speckle noise calculated by Eq. (6). (b) Frequency spectrum trend of the experimental speckle noise.

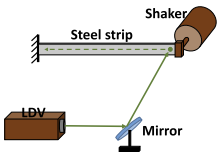


**Fig. 2.** Scheme of experiments.

trend of the frequency curve with oscillation period $v_s/L$:

$$\begin{aligned} &\min_{a_0,b_0,\varphi} \quad (y_t(f) - y(f))^2 \\ &\text{s.t.} \quad y_t(f) = a_0 e^{b_0 f} \sin\left(\frac{v_s}{L} f + \varphi\right) \\ &a_0,\ b_0 \in [-\infty, \infty],\ \varphi \in [0, 2\pi],\ f \in [f_\tau - f_0, f_\tau + f_0] \\ &\text{Output: } y_t(f_\tau), \end{aligned} \tag{7}$$

where $y_t(f)$ is the optimized curve trend in the moving window $f \in [f_\tau - f_0, f_\tau + f_0]$, $2f_0$ is the window length, and the frequency curve trend at each point $f_\tau$ is acquired by this optimization.

**Results**. Two experiments are conducted to evaluate the two despeckling strategies. Figure 2 presents the experimental scheme. An LDV transmits laser beams deflected by a rotating mirror onto the surface of a steel strip. By controlling the mirror, the focusing spot moves along the scanning direction, and we keep the basic concept of LDVom, one-way continuously scanning for one time. The steel strip is mounted as a cantilever beam with the end excited by a shaker. The artificial excitation is predefined as a 500 Hz sinusoidal wave for conveniently evaluating the despeckling result. The first experiment is intended to test the LPF when the vibration frequency is lower than $v_s/2L$. Three scanning speeds of 20 m/s, 10 m/s, and 0.1 m/s are compared, with $v_s/2L$ = 15 kHz, 7.5 kHz, and 75 Hz, respectively. The sampling frequency is 102,400 Hz.

Figure 3 illustrates the original vibration signals and the despeckling results. The noise intensely fluctuates to distort the vibrations, and numerous signal drop-outs appear. As aforementioned, we feed the signals into an LPF with a cutoff frequency

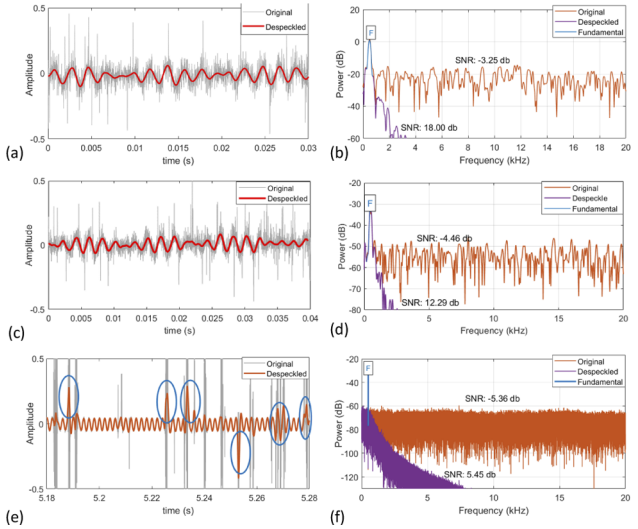


**Fig. 3.** (a) Original and despeckled signals with $v_s$ = 20 m/s. (b) Corresponding power spectrum of (a). (c) Original and despeckled signals with $v_s$ = 10 m/s. (d) Corresponding power spectrum of (c). (e) Original and despeckled signals with $v_s$ = 0.1 m/s. (f) Corresponding power spectrum of (e).

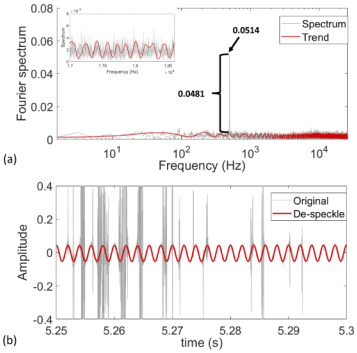


**Fig. 4.** (a) Fourier spectrum and the trend. (b) Original signal and the despeckling result between 5.25 s and 5.3 s.

of 700 Hz. With $v_s$ = 20 m/s and 10 m/s, the despeckling result has revealed a vibration around 500 Hz with time-variant amplitudes. The vibration curve visibly agrees well with the original signal trend, and the SNR increases to 21.25 db and 16.75 db, respectively. These results indicate the despeckling effectiveness. However, with $v_s$ = 0.1 m/s, the LPF result preserves numerous distortions (marked with blue ellipses) arising from the speckle noise, and the SNR only increases to 10.81 db. Therefore, the LPF is effective in eliminating the speckle noise if we control the scanning speed $v_s > 2Lf_v$ in the experiments, where $f_v$ is the vibration frequency.

The second experiment is designed to evaluate the other despeckling strategy, first extracting the oscillation trend [Eq. (7)] of the frequency curve and then removing this trend to acquire the actual vibration energy. The scanning speed is 0.1 m/s, and the sampling frequency is 102,400 Hz. The calculated frequency-peak interval of the Fourier spectrum is $v_s/L$ = 150 Hz. Two signal segments with weak and extremely weak vibrations are analyzed by the proposed approach.

Figure 4 illustrates the signals with vibration amplitudes around 0.05 and the corresponding Fourier spectrum. The vibration mode is visible in the Fourier spectrum. The original signal between 5.25 s and 5.3 s contains intense noise which nearly buries the vibrations. The LPF has poor performance in this situation as the intense noise results in large amplitude distortions [Fig. 3(c)]. First we calculate the spectrum trend according to Eq. (7). Despite the intense fluctuations, the spectrum fits well with the approximated trend [Fig. 4(a)]. Then, we cut off the spectrum with the trend and calculate the 500 Hz amplitude equaling 0.0481. If the spectrum is not cut off, the 500 Hz amplitude is 0.0514 with a 7% error, which would affect precise measurements. The signal time series is then reconstructed with the initial phase and the revealed amplitude. It reveals a vibration around 500 Hz, indicating the effectiveness in eliminating the speckle noise.

Figure 5 illustrates signals with extremely weak vibrations (amplitudes around 0.004) and the corresponding Fourier spectrum. The original signal between 4 s and 4.05 s contains intense noise. Similar to the above discussion, the frequency curve presents the trend with frequency-peak intervals of 150 Hz. The 500 Hz amplitude after cutting off the spectrum trend remains at 0.00397. If the spectrum is not cut off, the 500 Hz amplitude is 0.00498 with a 25% error, which is unacceptable. The reconstructed time series reveals the 500 Hz vibration, which fits well with the acquired signals. Therefore, the second despeckling strategy is effective regardless of the vibration intensity.

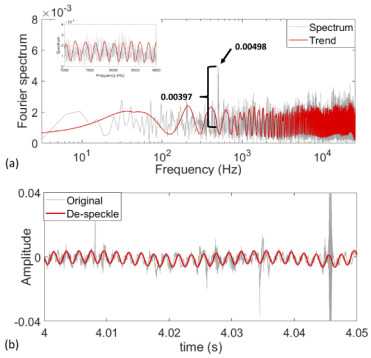


**Fig. 5.** (a) Fourier spectrum and the trend. (b) Original signal and the despeckling result between 4 s and 4.05 s.

**Conclusion**. In summary, two novel despeckling strategies have been proposed in this Letter according to Fourier properties. By theoretically conducting Fourier transform on the variation of the speckle phases, the frequency spectrum of the speckle noise presents oscillations with constant frequency-peak intervals. This agrees well with the experimental spectrum trend. Therefore, (1) an LPF can remove the noise if the vibration frequency is far lower than the first frequency peak of the speckle noise and (2) the vibration energy can be revealed by removing the oscillating frequency trend. The corresponding experiments have indicated that the two strategies based on Fourier analysis are effective in eliminating the speckle noise.

For the first strategy, the scanning speed should be the largest possible one according to Fig. 1, so that the noise level at $f_v$ is lowest. However, the scanning speed is also limited by the equipment ability, the scanning resolution required (e.g., if the resolution is 0.1 mm and the sampling frequency is 0.1 MHz, then the maximum scanning speed is 10 m/s), and so on. Therefore, the scanning speed is carefully chosen in real applications. Future development of digital equipment can improve the scanning ability.

We also mention that an infinite scanning series with random speckle patterns is assumed in theoretical analysis. This assumption would not affect the first strategy since the noise level is quite low with frequency less than $v_s/2L$. However, in a real situation with small-scale measurements, more fluctuations will appear in addition to the oscillating Fourier spectrum of speckle noise (Fig. 1). Thus the second strategy, which only removes the oscillating spectrum, will be affected.

In future applications, an LPF unit can be installed between the LDV and the signal acquisition instrument with fast scanning $v_s > 2Lf_v$. If the scanning speed limited by the equipment is improved, this strategy is more effective due to the simple LPF unit and possible realization of real-time despeckling. With $v_s \leq 2Lf_v$, the second strategy can complement the despeckling procedure in post-processing. However, this strategy is less effective with short time series or too many vibration modes. A more applicable strategy for short time series and many vibration modes should be investigated in future work.

**Disclosures.** The authors declare no conflicts of interest.

**Data availability.** Data underlying the results presented in this paper are not publicly available at this time but may be obtained from the authors upon reasonable request.

## REFERENCES


1. S. Sels, S. Vanlanduit, B. Bogaerts, and R. Penne, Mech. Syst. Signal Process. **126**, 427 (2019).
2. Y. Fu, M. Guo, and P. B. Phua, Opt. Lett. **35**, 1356 (2010).
3. T. Miles, M. Lucas, and S. Rothberg, Opt. Lett. **21**, 296 (1996).
4. P. Castellini, M. Martarelli, and E. Tomasini, Mech. Syst. Signal Process. **20**, 1265 (2006).
5. L. Chen, D. Zhang, Y. Zhou, C. Liu, and S. Che, Sci. Rep. **8**, 9094 (2018).
6. S. Rahimi, Z. Li, and R. Dollevoet, in *AIP Conference Proceedings, vol. 1600* (American Institute of Physics, 2014), pp. 274–286.
7. S. Rothberg, J. Baker, and N. Halliwell, J. Sound Vib. **135**, 516 (1989).
8. S. Rothberg, M. Allen, P. Castellini, D. Di Maio, J. Dirckx, D. Ewins, B. J. Halkon, P. Muyshondt, N. Paone, T. Ryan, H. Stegerh, E. P. Tomasinic, S. Vanlanduiti, and J. F. Vignolaj, Opt. Lasers Eng. **99**, 11 (2017).
9. Y. Jin and Z. Li, in *2021 13th International Conference on Measurement* (IEEE, 2021), pp. 72–75.
10. P. Martin and S. Rothberg, Opt. Lasers Eng. **47**, 431 (2009).
11. M. Martarelli and D. J. Ewins, Mech. Syst. Signal Process. **20**, 2277 (2006).
12. L. Pieczonka, L. Ambroziński, W. J. Staszewski, D. Barnoncel, and P. Pérès, Opt. Lasers Eng. **99**, 80 (2017).
13. P. Chiariotti, M. Martarelli, and G. Revel, Opt. Lasers Eng. **99**, 66 (2017).
14. J. Zhu, Y. Li, and R. Baets, Opt. Lett. **44**, 1860 (2019).
15. Y. Xu, D.-M. Chen, and W. Zhu, J. Sound Vib. **485**, 115536 (2020).
16. J. W. Goodman, "Statistical properties of laser sparkle patterns," Tech. rep. (Stanford Electronics Labs, Stanford University, 1963).
17. J. W. Goodman, Opt. Commun. **14**, 324 (1975).
18. S. J. Kirkpatrick, D. D. Duncan, and E. M. Wells-Gray, Opt. Lett. **33**, 2886 (2008).
19. J. C. Dainty, *Laser Speckle and Related Phenomena*, Vol. 9 of Topics in Applied Physics (Springer Science & Business Media, 2013).
20. J. W. Goodman, *Speckle Phenomena in Optics: Theory and Applications* (Roberts and Company Publishers, 2007).